International Journal of Recent Trends in Engineering & Research
ISSN (ONLINE) : 2455 – 1457
IMPACT FACTOR : 4.101

The effect of textured surfaces on the performance of p-i-n GaAs grown on high index substrates (11N)

I. Zeydi[1], Z. Zaaboub[1,2], L. Sfaxi[1,2], R. M'ghaieth[1]

[1]*Université De Monastir, Laboratoire de Micro-optoélectroniques et Nanostructures (LMON), Monastir 5000, Tunisie*

[2]*Université de Sousse, Ecole Supérieure des Sciences et de Nanotechnologie de Hammam Sousse, Rue Lamine Abassi, 4011 H.Sousse, Tunisie*

Corresponding author: Imen Zeydi

Abstract-We report the effects of the surface morphology of highly doped p-i-n GaAs elaborated on high index GaAs substrates namely (111)A and (114)A, on the optical and the electrical properties.The studied samples were fabricated by Molecular beam epitaxy (MBE). The optical and electrical characterizations were investigated via photoluminescence (PL), Time-Resolved Photoluminescence (TRPL), photocurrent (PC) spectroscopy andcurrent voltage (IV). PL measurements showed different peak emissions which are more pronounced in the PL spectra of the sample grown on (111) A. The presence of the PL peak emissions was attributed to the arsenic vacancy defects that change into pairs of Ga vacancy and Ga antisite defects when the Arsenic pressure is high. This result is attributed to the orientation dependence of the surface bonding and the kinetics of the MBE growth process. Moreover, a strong correlation between the PC measurement and carrier lifetime was observed, which is attributed to efficient photocarrier generation in the active layer of thecells. This is due to the presence of photo-generated carrier transfer from defect levels, induced by growth process, to the GaAs spacer layer. The (IV) characteristics in dark and illumination conditions show aninteresting results.

Keywords: III-V Solar cell, molecular beam epitaxy, high index substrates, textured surfaces

I. INTRODUCTION

P-i-n GaAs solar cells grown on (100) oriented GaAs substrates were quite investigated [1, 2, 3]. However, there is an utter lack regarding the properties of p-i-n GaAs grown on substrates other than the conventional (100) orientation. Recently, interest in the use of high index substrates has increased [4, 5, 6]. It was shown that the growth of GaAs on high index substrates relies on the growth parameters [7,8].These substrates exhibit a piezoelectric field that can be added to the internal electric field of the solar cell and consequently accelerate the spatial charge separation.

Over the last few years, the record energy-conversion efficiency for gallium-arsenide (GaAs) solar cells has broken 40% threshold and continues to increase [9]. Primarily, the choice of GaAs was attributed to its high electron mobility, its direct forbidden band and the good control of its mechanisms during MBE growth [10]. So as to acquire the best yield from GaAs devices, several suggestions have been reported just as the inclusion of multi stacked layers of InAs quantum dots within the intrinsic region. [11, 12, 13]. Others put forward the use of the non- GaAs substrates instead of the conventional one (001) [14].

Irrespective of the goal to realize high quality GaAs devices, High Miller index surfaces have recently been proposed, in order to influence, through the substrates orientation, the growth mechanisms, surface kinetics, impurity incorporation and strain relaxation and to obtain new interfaces by growing on crystal orientations other than (001) [4,15].The regrowth on high index planes has led to a great benefit for the research due to its prominence in the formation of advanced

quantum structures such as quantum wires and quantum dots [4, 5,6]. Besides, the epitaxial layers elaborated on high index surfaces depict a step forward in photovoltaic application, by dint of their piezoelectric field that amends the energy band structure, which causes a significant change in the optical proprieties [5, 6]. Choosing a piezoelectric field in the same direction as the one created by the p-n junction (internal field), the spatial separation of carriers is accentuated which improves the performance of solar cells.

In this context, we report the effect of elaborating p-i-n GaAs structures on high index substrates for photovoltaic applications. Photoluminescence (PL), time-resolved photoluminescence (TRPL), photocurrent spectroscopy (PC) and current voltage (I-V) are performed to investigate any enhancement due to the high index surfaces exploitation. The obtained results may offer new perspectives on the expansion of high III-V solar cells.

II. EXPERIMENTAL DETAILS

Two samples were grown by solid-source molecular beam epitaxy (SS-MBE) on n^+ GaAs (111) A and (114) A oriented substrates. Samples were bonded side by side on the same substrate holder in order to render them comparable (Figure 1 shows a schematic diagram of the structure).

Before the growth, the substrates were heated in-situ at 600°C where the thin oxide film was desorbed under As_4 flux bombardment. In situ, the morphology evolution was monitored by recording the intensity's evolution of the reflection high energy electron diffraction (RHEED). When a clear reconstruction appeared, the temperature was then increased to 620°C. The structures included 250 nm n^+ doped GaAs buffer ($4.55x10^{18}$ cm^{-3}) followed by a 1000 nm n doped GaAs base layer ($4.33x10^{17}$ cm^{-3}) . A further 245 nm semi insulting GaAs was then grown. The structures were completed by the addition of 250 nm p-GaAs emitter layer ($2.9x10^{18}$ $cm^{-}3$) accomplished by 100 nm p^+ GaAs contact layer ($3.4x10^{19}$ cm^{-3}) . We call S1 the cell grown on (111)A and S2 the cell grown on (114)A.

Silicon (Si) and Beryllium (Be) were used respectively as n and p type dopants. All the doping densities were determined by Hall Effect. The growth rate for GaAs layers was 2.19 Å/s. In order to check the growth, the temperature was calibrated by a pyrometer.

Photoluminescence (PL), time-resolved photoluminescence (TRPL), photocurrent (PC) and current-voltage (I-V) are widely used in semi-conductors characterization. In fact the material proprieties can be easily assessed. In (PL), an Argon (Ar^+) laser with a wave length of 514.5 nm was used as an excitation source to generate electron-hole pairs. The excitation density power was 100 W/ cm^2. The luminescence light from the samples was dispersed by a high-resolution spectrometer and detected by a thermoelectrically cooled InGaAs photo-detector with a built-in amplifier. The measurements were executed at low temperature (12K) and at room temperature (300K).

Time decays were measured using time-correlated single photon counting (Time- Harp, Pico Quant). The samples were excited by 781 nm picoseconds pulses generated by a Pico Quant, LDH-781 laser head, controlled by a PDL-800B driver. The setup was operated at an overall time resolution of ~30 ps. Decays were measured at the peak emission and reconvoluted using non-linear least squares analysis (FluoFit, Pico Quant). The accuracy of fit was judged in terms of χvalue (with a criterion of less than 1.1 for an acceptable fit) and weighted residuals.

The photo current measurements were investigated as a function of the wavelength. Indium zinc (InZn) alloy was used for the top ohmic contact and indium (In) for the bottom contact. The measurements were performed at 300 K using a photocurrent spectroscopy bench comprising a 100 mW tungsten halogen lamp, CVI CM110 1/8 monochromator and a keithley 6485 picoammeter.

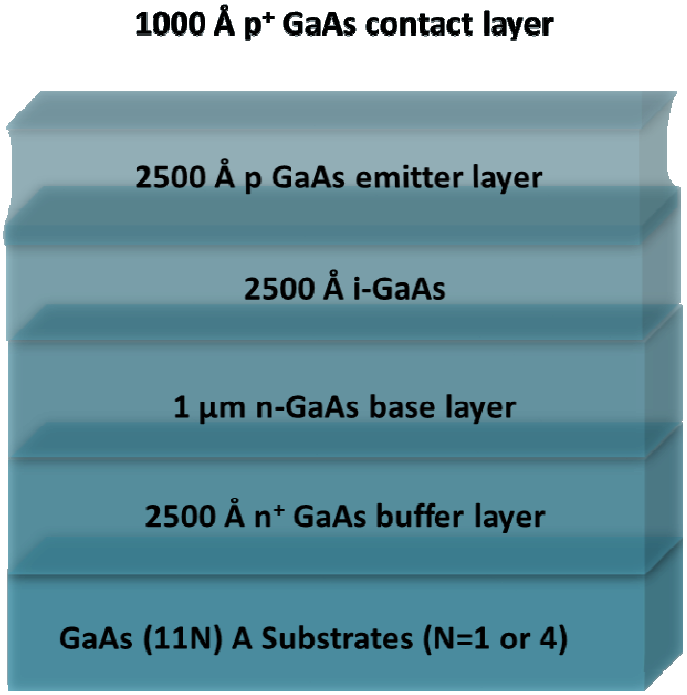

Fig 1. Schematic layers of the solar cells grown on (11N) n+ GaAs substrates

III. RESULTS AND DISCUSSION

Typical AFM images of surface morphology grown on GaAs (111) A and (114)A substrates are shown in Fig.2

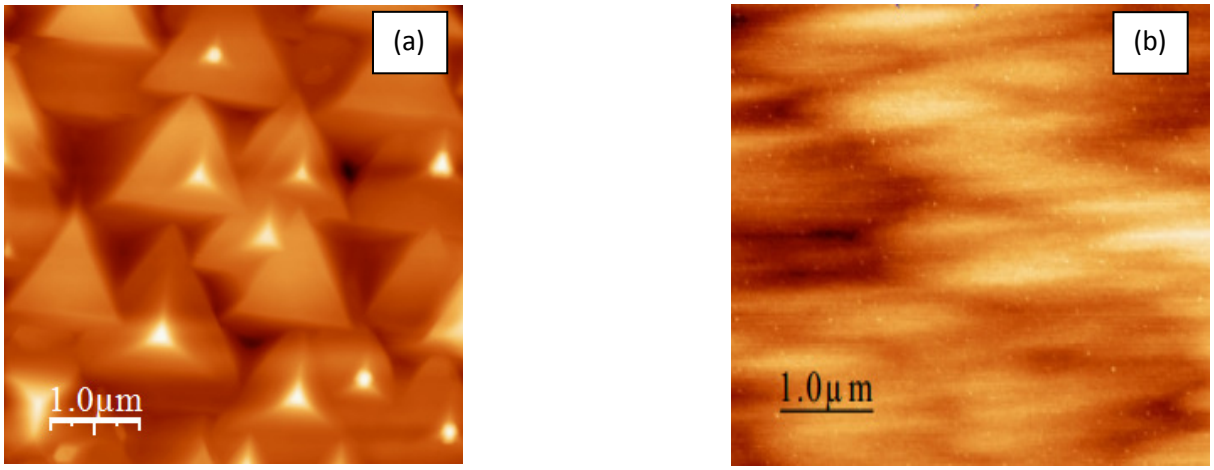

Fig.2. AFM images of p-i-n GaAs grown on: (a) (111) A, (b) (114) A at TAs= 195°C

The (111) A surface shows trigonal pyramids in which the three sidewalls had equivalent crystallographic faces. This observation suggests that the surface smoothness of the (111) A was improved by the effect of the Arsenic vapor pressure. The pyramids density was $2x10^{9}$ cm^{-2}. However the (114) surfaces are always perfectly plane and the crystallographic faces completely disappear.

This texturing has a double advantage. Indeed, when this surface is illuminated with a light of wavelength inferior to the dimensions of these pyramids, the light rays follow the laws of geometrical optics. The insertion on the Fig.3 presents the principle of multiple reflections proper to texturing. The relief of the surface causes a reduction in the reflection on the front face: a ray arriving at a normal incidence (relative to the plane of the cell) on a pyramid will be reflected on the

face of an adjacent pyramid, this double reflection on the pyramids decreases the total reflection coefficient, which is no longer R but R^2. On the other hand, a normal incidence ray will be transmitted in the cell with a refraction angle θ different from 0°. The path of this ray within the GaAs will therefore be increased by a factor of 1/sinθ with respect to the case of a plane surface perpendicular to the illumination, which will increase the photon fraction absorbed by the material. The second advantage of this texturing is to increase the area of the cell exposed to light. This leads to a more important trapping of the light penetrating into the cell

Fig.3 (a) shows the low temperature PL spectra of S1 grown on GaAs (111) A substrates. The PL spectra exhibit an emission peak with the highest intensity at about 1.48eV. This latter can be attributed to the recombination of electrons in the renormalized conduction band, with holes on deep acceptor levels. The association of this emissions with a point defect is also strongly suggested.In the shoulder of the strong PL signal around (1.50 eV), an emission was donated to the Ga_{As} (gallium anti-site defect). By comparison with the expected peak position of the band-to-band (e-h) emission in n-type defect-free GaAs of 1.52 eV [16], we can deduce an acceptor binding energy of about 0.045-0.05 eV. This level can be a Ga_{As}, which has a neutral charge state level at about 0.048 eV over the valence band maximum [17].Additional peak is observed at about and 1.53 eV. This sample hasa carrierconcentration $n>10^{18}$ cm^{-3}. For such a high free carrier concentration, previous works [16, 17] reported a luminescence band originated to the recombination of the degenerate electron gas with the holes in the valence band at about 1.52eV, with a slight reliance of its energy position on the free carrier concentration [16].
In addition, a broad but weak band emission centered at about 1.23 eV, was observed. This broadband emission is commonly related to the defect emission and probably due to Ga vacancies (V_{Ga}) [18] or clustering of Si atoms around a point defect [19].
Fig.3 (b) displays the PL spectrum at room temperature. The identified emission peaks in Fig.4 (a) are almost present with a slight red shift. We notice that the asymmetrical aspect is due to high doping.

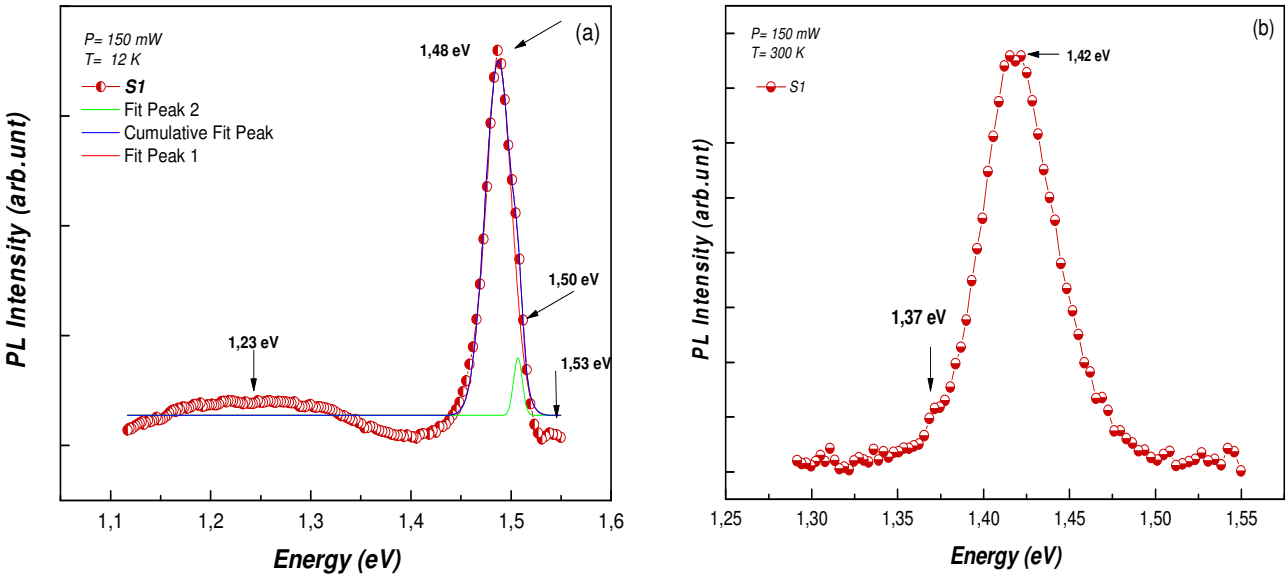

Fig.3. PL spectrum measured at low (a) and room temperature (b) for sample S1

Fig.4 illustrates the PL spectra of S2, at a low temperature (a) and room temperature (b). The images indicate the presence of three peaks (Fig.4 (a)). The first is associatedto the recombination of electrons in the renormalized conduction band, with holes on deep acceptor levels. The second is

attributed to Ga_{As} at ~1.43 eV, which is referred to the low arsenic (As) fluxes (we remind that the arsenic flux of S1 is still feeble compared to other studies [7]). At ~1.22 eV, the emission is associated to the gallium vacancies level (V_{Ga}). The peak revealed in (Fig.4 (b)) at ~1.41 eV, however, is attributed to the GaAs band gap emission.

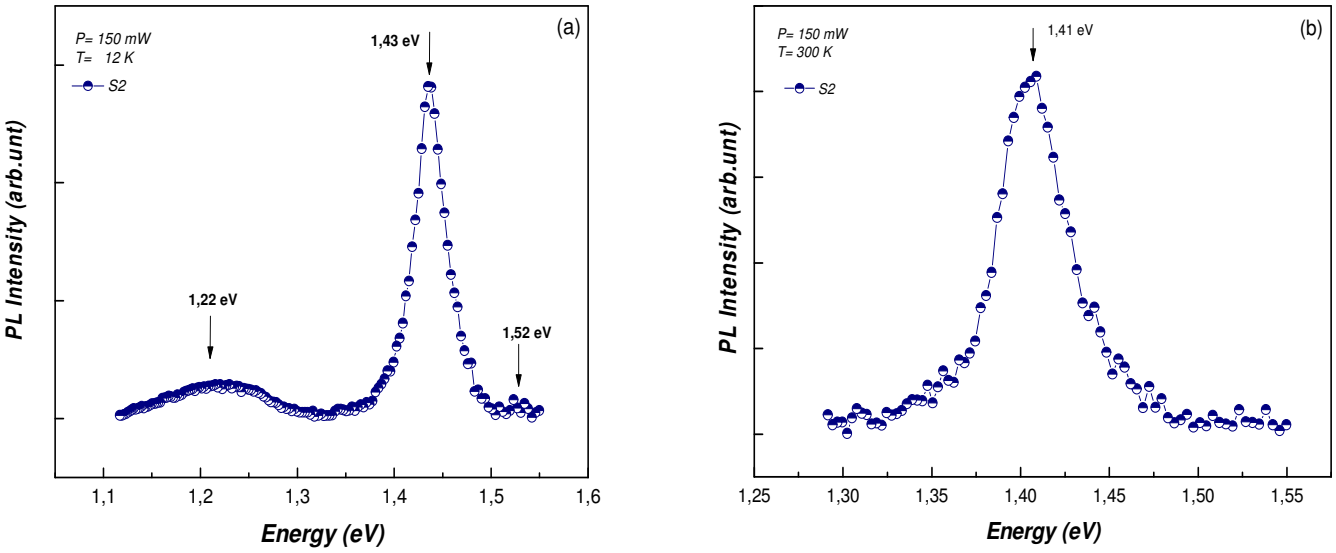

Fig.4. PL spectrum measured at low (a) and room temperatures (b) for samples S2

Time-resolved PL (TRPL) is one of the most powerful methods to understand the dynamics of carriers in semiconductors. It can estimate the minority carrier lifetime from the decay time of band-to-band recombination and carrier dynamics via localized levels and trap states in the active layer of solar cell devices [20]. This important parameter offered from the TR-PL characterization is essential to control the performance of such optoelectronic device.

However, at a low-temperature, in which the doping levels dominate, the characterization of the minority carrier lifetime is quite hard. Thus, TRPL measurements were performed at room temperature, in which band-to-band transition can be a measure for the recombination of minority carriers. Moreover, the ideal temperature for optoelectronic device operation is the room temperature.

Fig.5 shows the PL decay curves, of the studied samples, measured at room temperature and at the band gap emission wavelength. For both samples, the decay of photoluminescence emission is in the nanosecond scale and the decaying part of the TRPL data was described by a mono-exponential decay function expressed as:

$$I(t) = A\exp(-{}^{t}/_{\tau}) \qquad (1)$$

Where τ reflects the minority carriers lifetime and A is the amplitude which implies the number of counts at the end of the excitation.

Carriers lifetime obtained from data's fits are presented in Fig.5.The PL lifetime of sample S1 (3.52ns) is longer than S2. The measured decay time in S1 is around 4 times stronger than S2. The slow PL decay time evaluated for sample S2 suggests the re-excitation of the minority carriers before they recombine [21]. This result is mainly explained by the increase of the trapping rate into the nonradiative recombination process occurring in the defect states, resulting from an increase in carrier lifetime. In fact, it has been demonstrated that the presence of V_{Ga} and Ga_{As} lowers the electron-hole recombination efficiency, which is in good agreement with the (PL) results [22].

Moreover, knowing that the diffusion length is the average distance a carrier moves along, before disappearing, by recombination [20]. The increase of minority carrier lifetime in sample S1 indicates the good collection efficiency of photo-generated carriers in active layer. This fact is not merelydue to the nature of the (111) surfaces, but also, as demonstrated by PL measurements, it may be due to presence of the multiple energy levels created by the doping and the growth conditions.

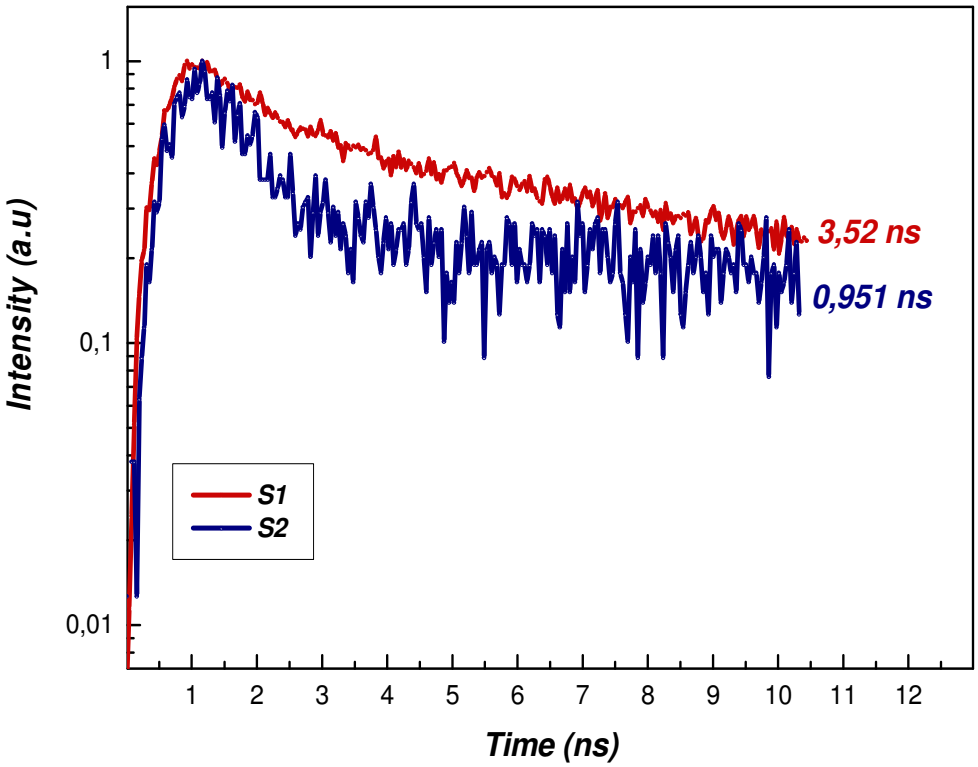

Fig.5. Normalized TRPL spectrum for S1 and S2

In Fig.6 (a) and (b), the photocurrent (PC) of all samples is shown. The curves have almost the same shape, however the maximum of the PC intensity changes. At the band gap of GaAs at (~866 nm), the PC responses of the homojunctions drop sharply indicating that the absorption of photons takes place only above the band-gap energy of GaAs (1.42 eV). An emission located at 1023 nm (1, 22 eV) due to the absorption from gallium vacancies level (V_{Ga}) (Fig.6). This latter was perceived in the PL measurements. We noticed thatthe photocurrent intensities are very remarkable. The measured photocurrent was equal to ~7 mA. As a matter of fact, the improvement in minority carrier lifetime produced an enhancement in the collection of photo-generated carriers.

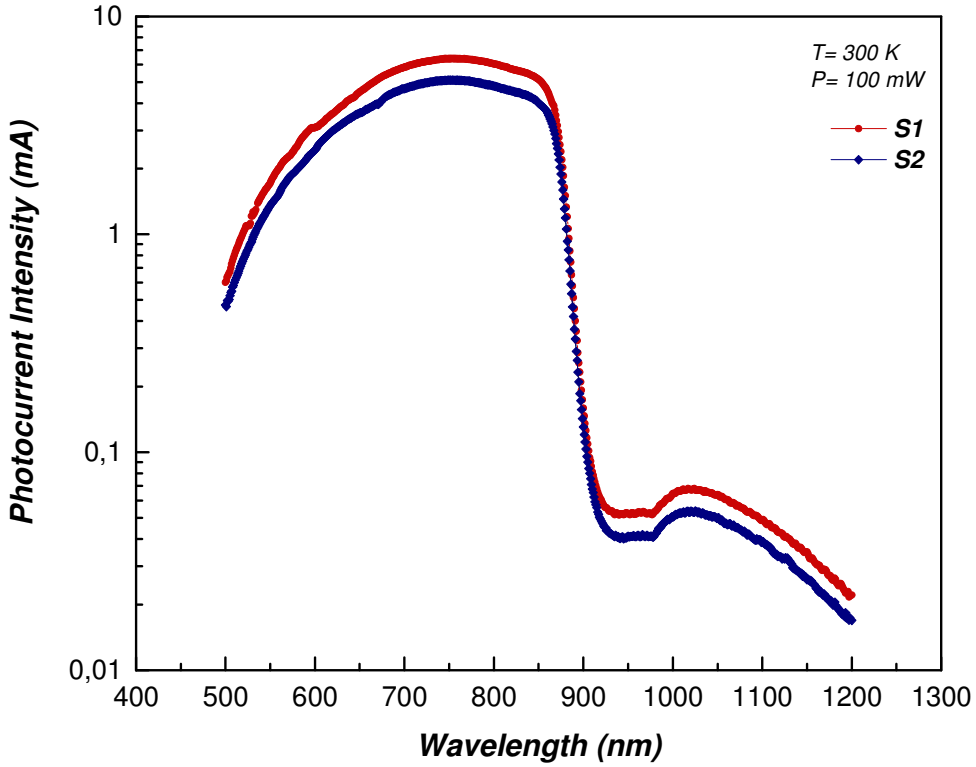

Fig.6.Photocurrent responses for S1 and S2s at room temperature

In figure 7, we performed the IV characteristic in both dark and illumination conditions.

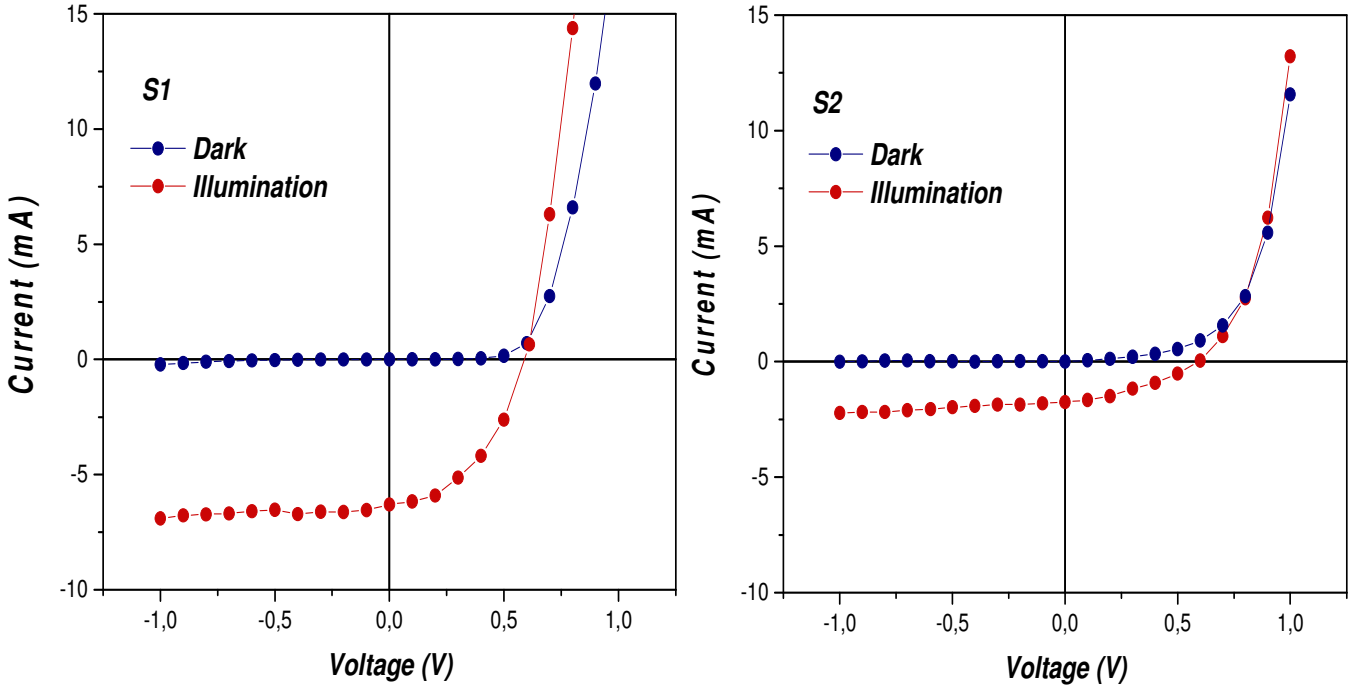

Fig.7. Current versus voltage characteristics for S1and S2 measured under dark and illumination conditions

Cell	R_S *(Ω)*	R_{Sh}*(Ω)*	V_{OC} *(V)*	I_{SC} *(mA)*
S1	7 .6	2050	0.6	6
S2	19	1993	0.59	1.763

Table.1. PV device parameters for S1 and S2

The basic photovoltaic device parameters extracted from the data are given in Table.1. It is noted that the photovoltaic quantities of S1 are significantly better than S2. The improvement is recorded mainly in the short-circuit current. By a comparison with a previous study done on the conventional GaAs, the measured I_{SC} was 1.5 mA [23]. While our results show a current 4 times stronger. With the use of (111)A substrates, the short-circuit current was increased to 6 mA and thereafter the yield. In fact, this result is attributed to the increase in the area exposed to light which is evident in the (111) orientation.

IV. CONCLUSION

To sum up, the present paper qualifies the impact of textured surface on the optical and the electrical properties of p-i-n GaAs grown on (111) and (114) orientations. There is a good correlation between the (TRPL) and PC measurements, where we have found that the best carrier lifetime and the photocurrent response are detected in S1.This improvement was primarily attributed to the texturedsurface of the (111) orientation.In fact the surface morphology influences on different characteristic parameters. Further exploitation of textured surfaces will provide a deeper improvement for photovoltaic applications.

ACKNOWLEDGMENT

The authors thank the Ministry of higher Education and Scientific Research (Tunisia).

Compliance with Ethical Standards

The authors declare that they have no conflict of interest.

REFERENCES

I. M.R. Melloch, S.P. Tobin, C. Bajgar, T.B. Sterllwag, A. Keshavarzi, M.S. Lundstorm, K. Emery, High-efficiency GaAs and AlGaAs solar cells grown by molecular beam epitaxy, *IEEE photovoltaic specialists conference* (1990), pp 163-167

II. N. Messei, M.S. Aida, numerical simulation of front graded and fully graded AlGaAs/ GaAs solar cell, *Optik* 126 (2015), pp 4432-4435

III. H. Urabe, M. Kuramoto, T. Nakona, A. Kawaharazuka, T. Makimoto, Y. Horikoshi, Effects of surface barrier layer in AlGaAs/ GaAs solar cells, *Journal of crystal growth* 425 (2015), pp 330-332

IV. M. Henini, Editorial, *Microelectronics journal*, 30 (1999), pp 313

V. M. Henini, Characterization and exploitation of epitaxial III-V compound semiconductor on novel index surfaces, Microelectronics journal, 26 (1995), pp 737-738

VI. M. Henini, Novel index surfaces workshop, *III-Vs Review*, 8 (1995), pp 42-44

VII. D. Johnston, L. Pavesi. M. Henini, Effect of As overpressure on Si-doped (111) A, (211) A and (311) A GaAs grown by molecular beam epitaxy, *Microelectronics journal*, 26 (1995), pp 759-765

VIII. T. Ohachi, M. Inada, K. Asai, J.M. Feng, Arsenic pressure dependence of hillock morphology on GaAs (n11) A substrates growing using MBE, *Journal of crystal growth*, 227-228 (2001), pp 67-71

IX. A.Luque and A. Marti, Increasing the Efficiency of ideal solar cells by photon Induced transitions at intermediate levels, *Phys. Rev. Lett,* 78 (1997), pp 5014-5017

X. J. Blakemore, Semiconducting and other major properties of gallium arsenide, *J. Appl. Phys*, 53 (1982), pp 123-181

XI. W. Rouis, M. Haggui, S. Rekaya. L. Sfaxi, R. M'ghaieth. H. Maaref, P. Fumagalli, Local photocurrent mapping of InAs/ InGaAs/GaAs using scanning near-field optical microscopy, *Solar energy materials and solar cells*, 144 (2016), pp 324-330

XII. A. Sayari, M. Ezzidini, B. Azeza, S. Rekaya, E. Shalaan, S.J. Yaghmour, A.A. Al-Ghamdi, L.Sfaxi, R. M'ghaieth, H. Maaref, Improvement of performance of GaAs solar cells by inserting self-organized InAs/ InGaAs quantum dot superlattices, *Solar energy materials and solar cells*, 113 (2013), pp 1-6

XIII. Al-Ghamdi, M.S, Sayari.A, Sfaxi.L, Optical study of high index substrate effect in multilayer InAs/GaAs quantum dot solar cells, *Journal of Alloys and Compounds*, 685 (2016), 202-208

XIV. B. Azeza, M.H.H. Alouane, B. Ilahi, G. Patriarche, L. Sfaxi, A. Fouzri, H. Maaref, R. M'ghaieth, Towards InAs/InGaAs/GaAs quantum dots solar cells directly grown on Si substrate, *Materials*, 8 (2015), pp 4544-4552

XV. M. Henni, S. Sanguinetti, L. Brusaferri, E. Grilli, M. Guzzi, M.D. Upward, P. Moriarty, P.H. Beton, Structural and optical characterization of self-assembled InAs-GaAs quantum dots grown on high index surfaces, *Microelectronics Journal*, 28 (1997), pp 933-938

XVI. G.borghs, K. Bhattacharyya, K. Deneffe, P. Van Mieghem, R. Mertens, Bandgap narrowing in highly doped n and p type GAAs studied by photoluminescence spectroscopy, *Journal of Applied Physics*, 66 (1989), pp 4381-4386

XVII. L. Pavesi, M. Guzzi, Photoluminescence of $Al_xGa_{1-x}As$ alloys, *Journal of Applied Physics*, 75 (1994), pp 4779-4842

XVIII. A. Amore Bonapasta, B. Bonanni, M. Capizzi, L. Cherubini, V. Emiliani, A. Frova, R.N. Sacks. F. Sarto, The spectrum of energy levels of the Ga-vacancy/ deuterium complexes in p-GaAs, *Journal of Applied Physics*, 73 (1993), pp 3326-3331

XIX. M. Suezawa, A. Kasuya, Y. Nishina, K.Sumino; Optical studies of heat-treated Si-doped GaAs bulk crystals, *Journal of Applied Physics*, 63 (1991), pp 1618-1624

XX. J. Bisquert, F. Fabregat-Santiago, I. Mora-Sero, G. Garcia- Belmonte, S. Giménez, Electron life in dye-sensitized solar cells : Theory and interpretation of mesurments, *J. Phys. Chem. C*, 113 (2009), pp 17278-17290

XXI. S. Shirakata, T. Nakada, Time-resolved photoluminescence in Cu (In, Ga) Se2 thin films and solar cells, *Thin solid films*, 515 (2007), pp 6151-6154

XXII. A. Jorio , C. Carlone, N.L. Rowell , A. Houdayer c M. Parenteau, Native defects in gallium arsenide grown by molecular beam epitaxy and metallorganic chemical vapour deposition: effects of irradiation, *Materials Science and Engineering B35* (1995),pp 160-165.

XXIII. W. Rouis , A.Sayari , N. Nouiri , M. Ezzdini, S. Rekaya, L. El Mir, L.Sfaxi, H. Maaref, Characterisation of the GaAs- based intermediate band solar cell with multi-stacked InAs/ InGaAs quantum dots, *Int.J.Nanotechnol*, (2015),pp 584-596.

